




# Geophysical Research Letters<sup>®</sup>



## RESEARCH LETTER

10.1029/2022GL101827

## Multistability and Transient Response of the Greenland Ice Sheet to Anthropogenic CO<sub>2</sub> Emissions

Dennis Höning<sup>1</sup> , Matteo Willeit<sup>1</sup>, Reinhard Calov<sup>1</sup>, Volker Klemann<sup>2</sup> , Meike Bagge<sup>2</sup> , and Andrey Ganopolski<sup>1</sup>

<sup>1</sup>Potsdam-Institute for Climate Impact Research, Potsdam, Germany, <sup>2</sup>Department of Geodesy, GFZ German Research Centre for Geosciences, Potsdam, Germany

### Key Points:

- Bifurcation points exist at global mean temperature anomalies of 0.6 and 1.6 K relative to pre-industrial
- Mass loss rate and sensitivity to cumulative CO<sub>2</sub> emission peak near the equilibrium ice volumes belonging to these temperature anomalies
- Substantial long-term mass loss of the Greenland ice sheet for cumulative emissions larger than 1,000 Gt carbon

### Correspondence to:

D. Höning,  
dennis.hoening@pik-potsdam.de

### Citation:

Höning, D., Willeit, M., Calov, R., Klemann, V., Bagge, M., & Ganopolski, A. (2023). Multistability and transient response of the Greenland ice sheet to anthropogenic CO<sub>2</sub> emissions. *Geophysical Research Letters*, 50, e2022GL101827. <https://doi.org/10.1029/2022GL101827>

Received 25 OCT 2022

Accepted 27 FEB 2023

**Abstract** Understanding the future fate of the Greenland Ice Sheet (GIS) in the context of anthropogenic CO<sub>2</sub> emissions is crucial to predict sea level rise. With the fully coupled Earth system model of intermediate complexity CLIMBER-X, we study the stability of the GIS and its transient response to CO<sub>2</sub> emissions over the next 10 Kyr. Bifurcation points exist at global temperature anomalies of 0.6 and 1.6 K relative to pre-industrial. For system states in the vicinity of the equilibrium ice volumes corresponding to these temperature anomalies, mass loss rate and sensitivity of mass loss to cumulative CO<sub>2</sub> emission peak. These critical ice volumes are crossed for cumulative emissions of 1,000 and 2,500 GtC, which would cause long-term sea level rise by 1.8 and 6.9 m respectively. In summary, we find tipping of the GIS within the range of the temperature limits of the Paris agreement.

**Plain Language Summary** With ongoing carbon dioxide emissions from the burning of fossil fuels, the atmosphere heats up, which has dramatic consequences for the ice sheets on Earth. In this study, we focus on the Greenland ice sheet (GIS), which holds so much ice that a complete melting would cause the global sea level to rise by 7 m. However, future mass loss of the GIS is challenging to predict because it is a non-linear function of temperature and occurs over long timescales. For this reason, we use CLIMBER-X, which is a coupled model of the whole Earth system. We find that the GIS features two critical volume thresholds, whose crossing would imply extensive further mass loss so that it would be difficult for the ice to grow back, even in thousands of years. Near these critical ice volumes, the mass loss rates are particularly high, and differences in the total carbon dioxide emission have a large impact. In summary, if cumulative emissions larger than 1,000 Gt carbon are released into the atmosphere, the GIS will shrink below a critical threshold and mass loss will inevitably continue until a substantial part of the ice sheet has melted.

## 1. Introduction

Between 2003 and 2016, the Greenland Ice Sheet (GIS) has lost mass at a rate of  $\approx 255$  Gt/yr (Mottram et al., 2019), with increasing atmospheric CO<sub>2</sub> from anthropogenic emissions expected to lead to further mass loss. Mass loss of the GIS is one of the main contributors to sea level rise (e.g., Aschwanden et al., 2019; Calov et al., 2018; Muntjewerf et al., 2020). Goelzer et al. (2020) estimate contributions of the GIS to global sea level rise ranging from  $32 \pm 17$  mm (RCP2.6 scenario) to  $90 \pm 50$  mm (RCP8.5 scenario) by 2100. An even higher rate of sea level rise would be expected for larger emissions and a corresponding higher global temperature rise (Applegate et al., 2015). In addition to sea level, freshwater flux from mass loss of the GIS affects the Atlantic Meridional Overturning Circulation (AMOC; e.g., Bakker et al., 2016; Yu et al., 2016). A substantial weakening or even a complete shutdown of the AMOC would have dramatic consequences for the environmental conditions on our planet, such as a strong cooling of the North Atlantic (e.g., Jackson et al., 2015) and possibly even have an impact on the stability of the Amazon rainforest (Ciemer et al., 2021). Hence, understanding the connection between anthropogenic CO<sub>2</sub> emissions and long-term GIS mass loss is of fundamental importance to predicting Earth's future environmental conditions.

The surface mass balance (SMB)–elevation feedback leads to a non-linear response of the GIS to temperature rise: an increase in surface melt results in widespread thinning at lower elevations. Thinning lowers the ice surface and exposes it to higher air temperatures, thereby leading to enhanced melt and further thinning. In equilibrium experiments, for which models are run with constant external forcing until the ice volume reaches an equilibrium, a small increase in temperature has been found to generally decrease the Greenland ice volume only

© 2023. The Authors.

This is an open access article under the terms of the [Creative Commons Attribution License](https://creativecommons.org/licenses/by/4.0/), which permits use, distribution and reproduction in any medium, provided the original work is properly cited.

to a small extent; however, if a critical threshold is crossed, the equilibrium ice volume can decrease substantially and would not recover even if global temperature declines again (Charbit et al., 2008; Ridley et al., 2010; Solgaard & Langen, 2012). Robinson et al. (2012) suggest the existence of multiple bifurcation points within a temperature anomaly of 2 K.

A connection between equilibrium states of the GIS and the rate of its response to anthropogenic CO<sub>2</sub> emissions exists. Similar to the equilibrium experiments, small cumulative emissions may only cause a relatively small and slow mass loss, but a crossing of critical thresholds (i.e., “tipping points”) may dramatically accelerate the latter (e.g., Armstrong McKay et al., 2022; Gregory et al., 2004; Gregory & Huybrechts, 2006; Irvali et al., 2020; Noël et al., 2017; Pattyn et al., 2018). Irvali et al. (2020) suggest that such a threshold lies between a temperature anomaly of 0.8 and 3.2 K.

Systematically investigating the long-term consequences of CO<sub>2</sub> emissions on mass loss of the GIS is challenging because of the relevant timescales in the order of thousands of years. The elevation of the ice sheet on these timescales can substantially evolve, affecting atmospheric dynamics and precipitation patterns. Accurately capturing these connections requires coupling of the ice sheet model with a climate model. However, complex Earth system models (ESMs) are too expensive to run over thousands of years, which motivates the use of ESMs of intermediate complexity (EMICs, Claussen et al., 2002). On the downside, the relatively coarse resolution of the ice sheet required to simulate long timescales likely underestimates the response time of the GIS to temperature forcing especially during the first centuries to millennia due to the not explicitly resolved interaction between outlet glaciers and the ocean (Aschwanden et al., 2016, 2019; Choi et al., 2021).

Using the EMIC LOVECLIM, Huybrechts et al. (2011) found an almost complete melting of the GIS within 3 Kyr for a constant atmospheric CO<sub>2</sub> concentration of 1,120 ppm. A constant CO<sub>2</sub> concentration, however, is not realistic. Using the updated version LOVECLIMv1.3, Van Breedam et al. (2020) studied the response of the GIS to cumulative emissions between 460 and 5,300 Gt carbon (GtC) and found an almost complete melting of the GIS within 10 Kyr for all emission scenarios. This result is contrary to the result of Charbit et al. (2008), who found a complete melting of the GIS only for cumulative emissions of 3,000 GtC or larger.

In this paper we use an EMIC with interactive GIS and atmospheric CO<sub>2</sub> to study the contribution of the GIS to future sea level rise on multi-millennial timescales for different CO<sub>2</sub> cumulative emission scenarios. For the first time, we connect transient experiments with equilibrium states of the GIS, and interpret future sea level rise from melting of the GIS using the stability diagram. We focus on values of the GIS volume for which a small perturbation would cause the system to leave its previous domain of attraction, and explore whether and how the mass loss rate changes as these specific values of the ice volume are crossed.

## 2. Methods

We use CLIMBER-X (Willeit et al., 2022, 2023), which is a fully coupled EMIC, including modules for atmosphere, ocean, land surface, sea ice and the 3-D polythermal ice sheet model SICOPOLIS v5.1 (Greve, 1997). SICOPOLIS is based on the shallow ice approximation for grounded ice, the shallow shelf approximation for floating ice and hybrid shallow-ice–shelvy-stream dynamics for ice streams (Bernales et al., 2017). The enthalpy method of Greve and Blatter (2016) is used as the thermodynamics solver. The ice sheet model is applied to the GIS at a horizontal resolution of 16 km and also includes a parameterization for small-scale ice discharge into the ocean through the numerous outlet glaciers (Calov et al., 2015), which cannot be explicitly represented in relatively coarse resolution continental-scale ice sheet models. A physically-based surface energy and mass balance scheme (SEMI, Calov et al., 2005) is used to interface the ice sheet model with the atmosphere. The glacial isostatic adjustment, which controls regional sea level change and surface displacements on the considered multi-millennial timescale, is computed by the viscoelastic lithosphere and mantle model VILMA (Bagge et al., 2021; Klemann et al., 2008; Martinec et al., 2018). CLIMBER-X also includes a detailed representation of the global carbon cycle, which allows to prognostically compute the atmospheric CO<sub>2</sub> concentration (Willeit et al., 2023).

In comparison to previous studies on the long-term fate of the GIS (Charbit et al., 2008; Van Breedam et al., 2020), the main advances in our modeling approach are (a) the fully coupled climate–ice sheet–carbon cycle model setup, including prognostic atmospheric CO<sub>2</sub>, and (b) the use of a physically based surface energy and mass balance interface instead of the positive degree day approach used for ablation in previous works.

A comparison of the SMB from historical runs with CLIMBER-X using prescribed ice sheets with regional climate models (RCM) is shown in Appendix A. While the integrated SMB of the GIS is in good agreement

with estimates from RCMs, there are differences in the spatial pattern of the simulated SMB, with CLIMBER-X underestimating SMB along the south-east coast and overestimating SMB in the north-east and south-west of the GIS. A comparison of the spatial extent and elevation of the pre-industrial GIS used in our transient experiments with the present-day observed ice sheet shows reasonable agreement (Appendix A).

We distinguish two experimental settings with the aim to discuss long-term committed sea level rise due to volume loss of the GIS in relation to the stability diagram of the latter. In the first setting, we prescribe a constant atmospheric CO<sub>2</sub> concentration between 200 and 500 ppm and run the model until it reaches a quasi-equilibrium ( $dV/dt < 1$  mm sea level equivalent (sle) Kyr<sup>-1</sup>, averaged over 10 Kyr) in order to trace the stability diagram of the GIS in a phase space spanned by atmospheric CO<sub>2</sub> concentration (or global surface air temperature) and ice volume. We use four different initial conditions, corresponding to the pre-industrial state, an ice-free Greenland, and two intermediate states resulting from previous simulations (see Section 3). In the second setting, we explore the effect of cumulative CO<sub>2</sub> emissions on the transient future GIS evolution. In this setting, we initialize the GIS elevation from present-day observations with a uniform ice temperature of  $-10^{\circ}\text{C}$  and first let the model run for 10 Kyr, allowing the ice sheet to reach a quasi-equilibrium. We then introduce cumulative emissions between 0 and 4,000 GtC, evenly spread throughout a time interval of 100 years, and explore their impact on the ice sheet volume for the following 20 Kyr. In this setting, CLIMBER-X is run in a fully coupled setup with interactive GIS and interactive atmospheric CO<sub>2</sub>. The orbital configuration is fixed at its present-day state. We allow for a carbon sink due to silicate weathering and set the volcanic outgassing rate constant to balance silicate weathering at pre-industrial conditions (Willeit et al., 2023).

### 3. Results

We start by presenting results of the GIS stability analysis for constant atmospheric CO<sub>2</sub> in Section 3.1 followed by transient experiments for different CO<sub>2</sub> emission scenarios in Section 3.2.

#### 3.1. Stability Diagram of the Greenland Ice Sheet

The stability diagram (Figure 1) presents equilibrium states of the GIS as a function of atmospheric CO<sub>2</sub> concentration for initial conditions of a pre-industrial GIS (blue curve) and a completely ice free GIS (red curve). The strong decrease of the ice volume between A and B and between C and D indicates the existence of bifurcation points at the corresponding CO<sub>2</sub> values. We then run simulations where we start with the GIS corresponding to points B and D and connect the obtained equilibrium points for lower CO<sub>2</sub> concentrations with a yellow and purple curve, respectively. Altogether, between a temperature anomaly of 0 and 2 K, we identify four equilibrium branches of the GIS, with equilibrium ice volumes that depend on their initial state.

Starting from pre-industrial GIS, the first bifurcation point (Figure 1, point A) corresponds to a temperature anomaly of 0.6 K (CO<sub>2</sub> level of 320 ppm). In equilibrium, the GIS at a global temperature anomaly of 0.6 K has a volume anomaly of  $\Delta V_A = -0.26$  m sle compared to the pre-industrial GIS. This suggests that, since the 1950s when the atmospheric CO<sub>2</sub> concentration crossed 320 ppm, the GIS has been far from an equilibrium state. Starting from this equilibrium point A, a further temperature increase would cause the GIS to approach a new equilibrium with an ice volume anomaly of  $-1.8$  m sle (point B). If the GIS reaches point B due to a temperature anomaly  $>0.6$  K, it would not return to point A even if the temperature anomaly would be reduced to 0.6 K. The second bifurcation point refers to a temperature anomaly of 1.6 K (400 ppm atmospheric CO<sub>2</sub>) and  $\Delta V_C = -2.4$  m sle, where the south of the GIS is melted (point C). A further temperature increase would cause the system to approach a new equilibrium where ice only remains in the north-east of Greenland (point D). If the GIS reaches this state, reducing atmospheric CO<sub>2</sub> would cause the GIS to follow the purple curve, meaning that the ice would not grow back substantially until atmospheric CO<sub>2</sub> concentration is reduced to 300 ppm or less. If the entire GIS is melted, regrowth of the bulk of the GIS would require an atmospheric CO<sub>2</sub> concentration below the pre-industrial level (red curve). Throughout the rest of the paper,  $\Delta V_A = -0.26$  m sle and  $\Delta V_C = -2.4$  m sle will be used for the two critical ice volume anomalies, which correspond to the equilibrium states of the system that belong to the bifurcation points A and C. We note that the resulting geometry of ice retreat differs from previous studies: in our simulations, the GIS starts to retreat from the south, whereas previous studies also find ice retreat in the north-west of Greenland (e.g., Huybrechts et al., 2011; Vizcaíno et al., 2008).

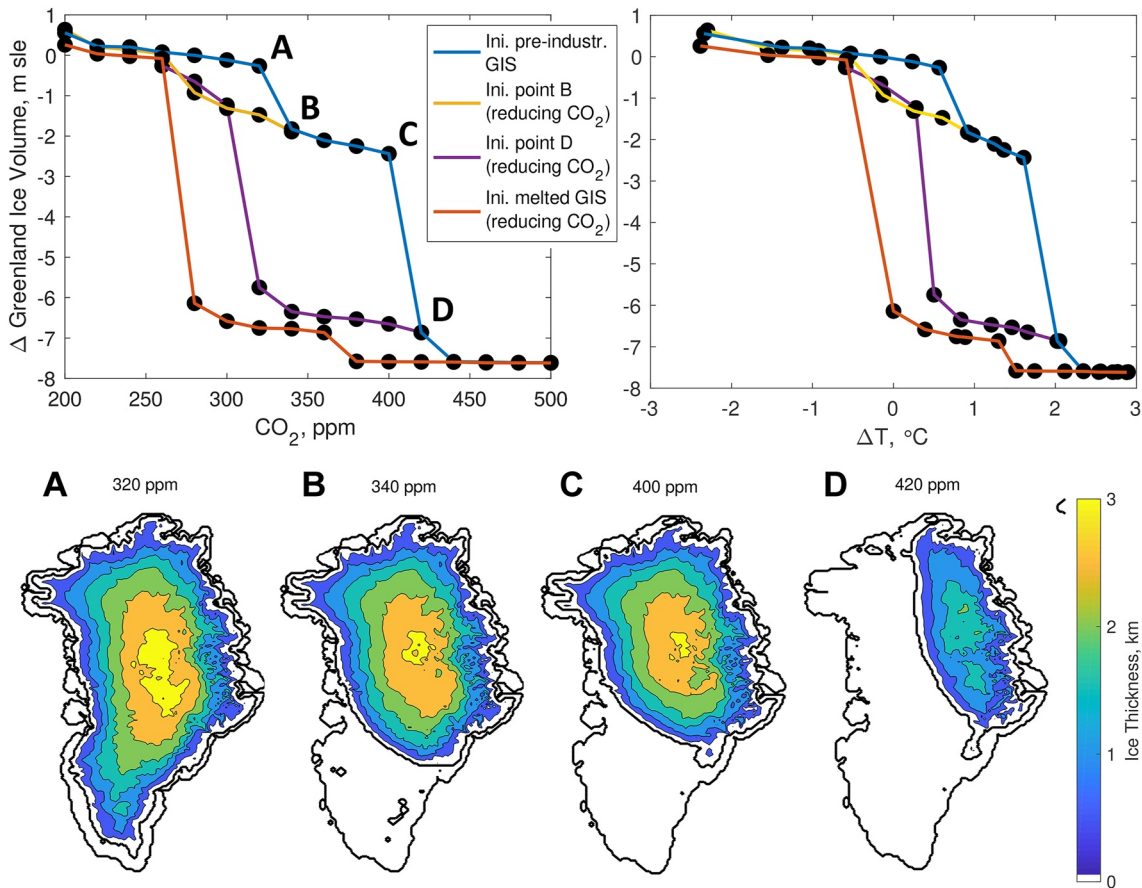


**Figure 1.** Equilibrium states of the volume of the Greenland Ice Sheet (GIS) (black dots) with respect to pre-industrial as a function of atmospheric  $\text{CO}_2$  concentration (top left) and corresponding temperature anomaly (top right). The blue curve refers to increasing  $\text{CO}_2$  concentration starting from the pre-industrial GIS, the other curves to decreasing  $\text{CO}_2$  starting from a completely ice free GIS (red curve) and from intermediate states (yellow and purple curves), respectively. The bottom panel illustrates the GIS thickness at the points A–D.

### 3.2. Transient Response of the Greenland Ice Sheet to Anthropogenic $\text{CO}_2$ Emissions

Reaching an equilibrium of the GIS requires a constant level of atmospheric  $\text{CO}_2$  over thousands of years, which is not realistic because oceans will slowly take up carbon from the atmosphere. The carbonate–silicate cycle will slowly cause the atmospheric  $\text{CO}_2$  to evolve back to its pre-industrial value, even though this will take hundreds of thousands of years. In this section, we explore a connection between the stability diagram of the GIS that has been discussed in Section 3.1 and transient simulations driven by anthropogenic  $\text{CO}_2$  emission scenarios in which the atmospheric  $\text{CO}_2$  concentration is modeled interactively.

Figures 2a–2c present the decline of atmospheric  $\text{CO}_2$  after the emission pulse over 10 Kyr and the resulting global temperature anomaly and volume of the GIS. Although the GIS is close to equilibrium when we introduce  $\text{CO}_2$  emissions, we still observe a slight drift of ice volume in the reference simulation at a rate of  $\approx 1 \text{ cm sle Kyr}^{-1}$  (Figure 2c, top green curve). In our simulations with cumulative emissions below 1,000 GtC, the GIS loses volume only during the first 1,000 years, if at all, and then ice starts to regrow (Figures 2c and 2d). For cumulative emissions larger than 1,000 GtC, the GIS continues to lose volume throughout the course of the entire experiment, although a substantial fraction of the loss occurs within the first 1 Kyr. For 10 Kyr and  $>1,000 \text{ GtC}$  cumulative emissions, the committed GIS contribution to sea level rise strongly and nonlinearly depends on the cumulative emissions. We note that 1,000 GtC leads to a higher final  $\text{CO}_2$  concentration than 1,250 GtC in our simulations. Additional experiments have shown that this result is attributed to a non-linear response of the  $\text{CO}_2$  uptake and overturning rate of the Southern Ocean to global warming.

As expected, trajectories in the volume–temperature phase space of the GIS (Figures 2e and 2f) first show increasing temperature at roughly constant ice volume during the emission phase. After that, the trajectories



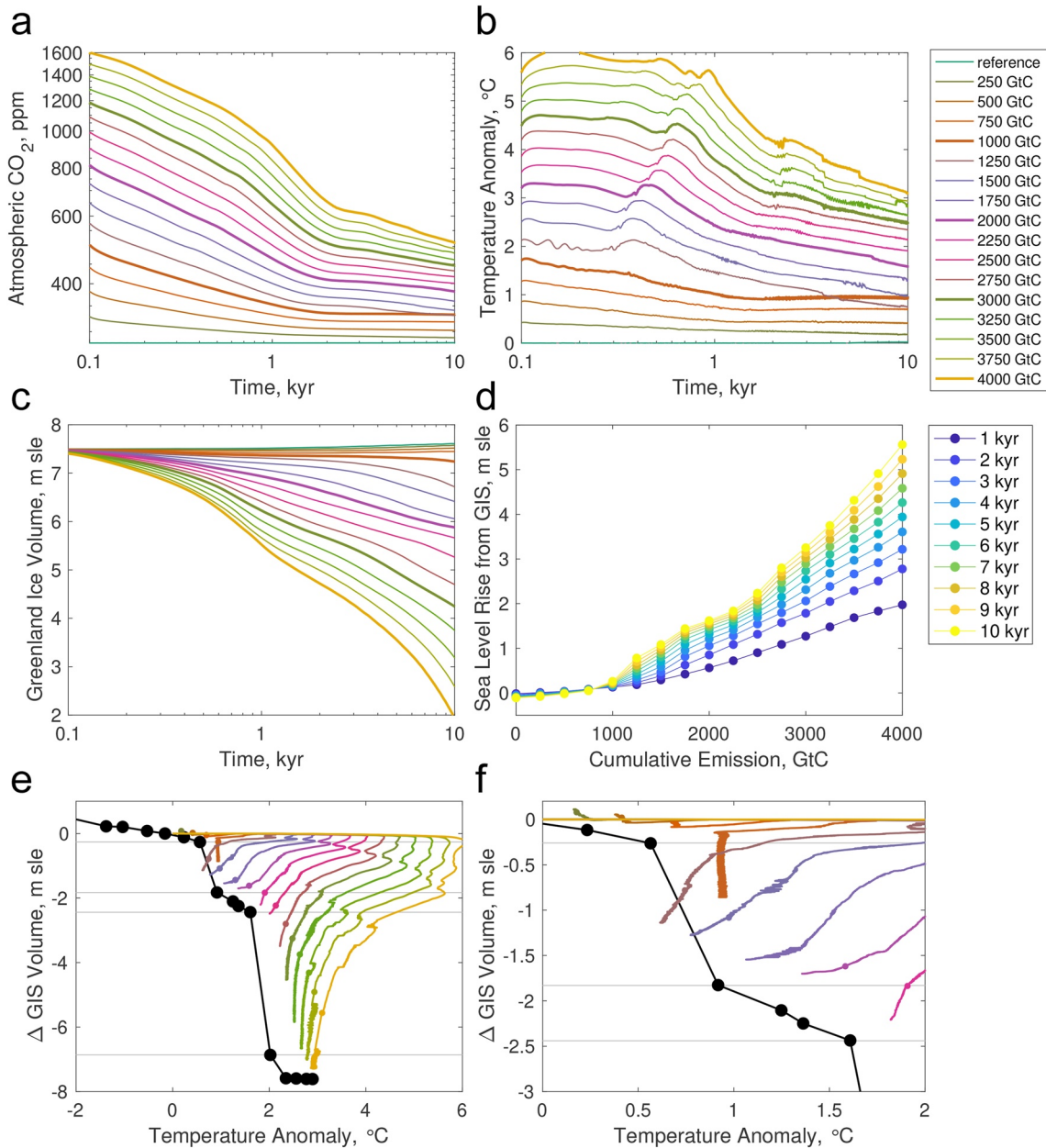


**Figure 2.** Transient results for cumulative emission scenarios between 0 and 4,000 GtC in steps of 250 GtC introduced throughout a time interval of 100 years. (a) Atmospheric CO<sub>2</sub> concentration, (b) global annual surface air temperature anomaly relative to pre-industrial, (c) Greenland Ice Sheet (GIS) volume, (d) sea level rise from GIS mass loss as a function of the cumulative CO<sub>2</sub> emission for different snapshots in time. Panels (e) and (f) show evolution trajectories over 20 Kyr (small colored dots indicating the state after 10 Kyr) and equilibrium states of the GIS (black dots) for model runs that start from pre-industrial GIS (Figure 1, blue curve). In (e) and (f),  $\Delta V_A \dots \Delta V_D$  are indicated as thin, gray horizontal lines.

show decreasing temperature and ice volume. The trajectories clearly show that a temporal overshoot of the critical temperature thresholds  $\Delta T_A$  (which is the temperature anomaly at point A) or  $\Delta T_C$  does not necessarily imply a crossing of the critical ice volumes  $\Delta V_A$  (which is the ice volume anomaly at point A) or  $\Delta V_C$ . Therefore, a temporal overshoot of a critical temperature does not necessarily lead to long-term ice loss (see also Ritchie et al., 2021). For example, in the case of relatively moderate emissions (750 GtC), the temperature anomaly is larger than  $\Delta T_A = 0.6$  K for more than 10 Kyr, after which it returns below the critical threshold  $\Delta T_A$ . However, the  $\approx 10$  Kyr long overshoot of the bifurcation temperature is still not sufficient to cause an ice mass loss larger than  $\Delta V_A$ , which would be required in order to cause the system to evolve towards the new equilibrium branch.

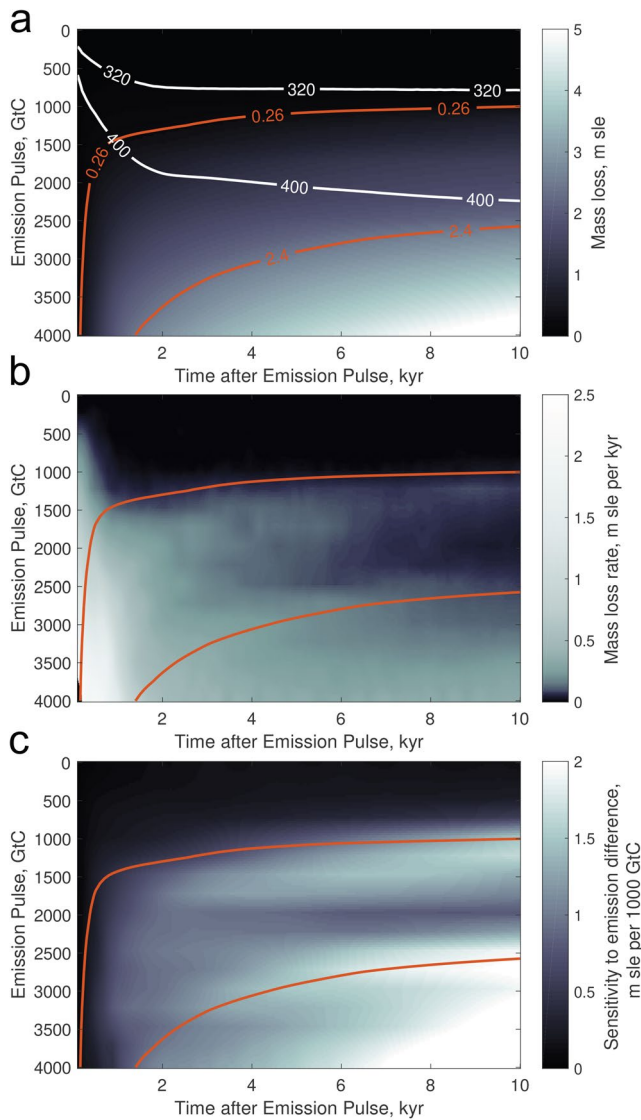


**Figure 3.** Total mass loss (a), mass loss rate (b), and mass loss sensitivity to differences in the cumulative emission (c). The red and the white curves depict the critical ice volumes  $\Delta V_A$  and  $\Delta V_C$  and the corresponding atmospheric  $\text{CO}_2$  of the bifurcation points, respectively. We note the non-linear colorscale in panel (b); the highest mass loss rates are found within the first 1 Kyr.

We observe a relationship between the equilibrium branches and the trajectories: While trajectories in Figures 2e and 2f have a small slope at ice volumes within the interval of the equilibrium branches, their slope is generally steeper in between these branches (at ice volumes between points A and B and between points C and D in Figure 1a). This result indicates that, as the ice volume anomalies  $\Delta V_A = -0.26$  m sle and  $\Delta V_C = -2.4$  m sle are crossed, the rate of mass loss increases.

In the following, we systematically explore connections between mass loss of the GIS and the critical ice volumes  $\Delta V_A$  and  $\Delta V_C$ . Figure 3 illustrates (a) the total mass loss  $m$ , (b) the mass loss rate  $dm/dt$  (where  $t$  is time), and (c) the sensitivity of mass loss to differences in the cumulative emission  $dm/dc$  (where  $c$  is cumulative  $\text{CO}_2$  emission). The ice volumes  $\Delta V_A$  and  $\Delta V_C$ , which correspond to bifurcation points in the equilibrium simulations, are depicted as red curves, and in Figure 3a, the respective atmospheric  $\text{CO}_2$  of the bifurcation points as white curves.

Whether (and at which time after the emission pulse) the GIS reaches the critical values  $\Delta V_A$  and/or  $\Delta V_C$  (red curves) is a function of cumulative  $\text{CO}_2$ . The minimum cumulative emission that leads to a crossing of  $\Delta V_A$  or  $\Delta V_C$  in the long term can be estimated by extrapolating the white and red curves in Figure 3a: whereas the red curve serves as a lower bound for the minimum cumulative emission (ice may continue to melt), the white curve serves as an upper bound, since the  $\text{CO}_2$  concentration needs to exceed 320 (or 400 ppm) in equilibrium to cross the respective bifurcation point. This indicates a minimum cumulative emission of approximately 1,000 and 2,500 GtC for crossing  $\Delta V_A$  and  $\Delta V_C$ , respectively.

The mass loss rate is particularly high in the first 1 Kyr. However, it also becomes apparent that the mass loss rate is generally high at ice volumes in the vicinity of the critical values  $\Delta V_A$  and  $\Delta V_C$  (red curves, Figure 3b). Furthermore, the sensitivity of mass loss to cumulative emission (Figure 3c) is particularly high in the vicinity of these critical ice volumes, too. In other words, differences in the cumulative emission of up to 1,000 GtC are of minor importance for mass loss of the GIS. However, when approaching  $\Delta V_A$ , differences in the cumulative emissions may be crucial for mass loss of the GIS, and a similar conclusion can be drawn for  $\Delta V_C$ . Altogether,  $\Delta V_A$  and  $\Delta V_C$  are critical volume anomalies of the GIS where mass loss is accelerated and increasingly sensitive to differences in the cumulative emission. In addition, crossing these critical ice volumes would imply that ice would not grow back to its previous state even if  $\text{CO}_2$  would be reduced accordingly.

#### 4. Discussion

Even if global warming is limited to  $1.5^\circ\text{C}$ , as recommended in the Paris agreement, several tipping points might already have been crossed (e.g., Armstrong McKay et al., 2022), and previous studies already have indicated that a critical threshold of the GIS is close to this value (e.g., Robinson et al., 2012; Van Breedam et al., 2020). We find two critical temperature anomaly thresholds above which the equilibrium volume of the GIS decreases non-linearly, at approximately  $0.6$  and  $1.6^\circ\text{C}$ . However, a temporary overshoot of these critical temperature thresholds does not inevitably cause long-term melt of the ice sheet (see Section 3.2). With transient experiments, we find that an equilibrium state of the GIS with smaller ice volume is approached only if the  $\text{CO}_2$  forcing is applied sufficiently long that the ice volume falls below the values of  $\Delta V_A = -0.26$  m sle and  $\Delta V_C = -2.4$  m sle, respectively.

Similar to the results of Robinson et al. (2012), we find multiple equilibrium states of the GIS. However, Robinson et al. (2012) found an intermediate equilibrium state where the northern part of the GIS is melted. In contrast,

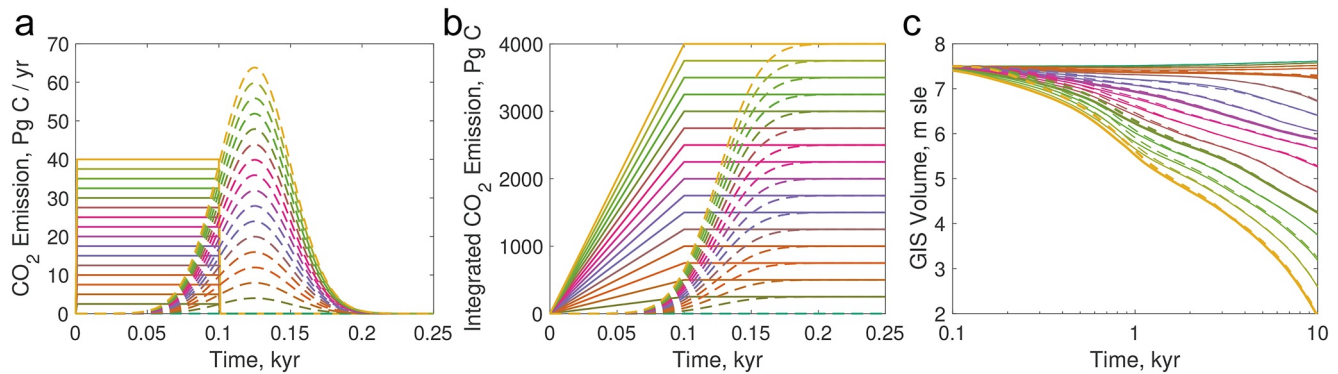


**Figure 4.** Comparison between constant emission rate over 100 years (solid) to a bell-shaped emission rate (dashed) for cumulative emissions between 250 and 4,000 GtC (color-coded as in Figure 2). (a) Emission rate, (b) cumulative emission, (c) Greenland Ice Sheet volume.

the results in the present paper indicate that at the intermediate equilibrium state the southern part of the GIS is melted. Satellite measurements of the gravity recovery and climate experiment GRACE during the recent years (<https://svs.gsfc.nasa.gov/31156>) show high mass loss rates particular in the south of the GIS, which indicates that our model results with CLIMBER-X are reasonable. We elaborate on the tendency of the GIS in our model to start lose mass from the south, as well as on a comparison to RCMs, in Appendix A. With further increasing CO<sub>2</sub>, our results indicate a small remaining ice volume in the east, which in turn is similar to the results of Robinson et al. (2012) (despite that no ice is left in the south of the GIS in our simulations).

Charbit et al. (2008) found a critical cumulative emission that would lead to a complete melting of the GIS between 2,500 and 3,000 GtC. This result is qualitatively similar to ours, where a cumulative emission of 2,750 GtC causes the ice volume to fall below the critical value (point C) after 10 Kyr. However, our results indicate that an additional equilibrium state (point D) exists, where a small part of the GIS remains in the east (compare Figure 1).

Contrary to our results, Van Breedam et al. (2020) found a complete melting of the GIS within 10 Kyr for cumulative emissions of only 460 GtC. The reason for this is twofold: on the one hand, the atmospheric CO<sub>2</sub> in our model decreases faster than in Van Breedam et al. (2020). On the other hand, even for a temperature anomaly of  $\approx 1.5$  K over 10 Kyr, Van Breedam et al. (2020) obtained almost a complete melting of the GIS, whereas only the south of the GIS has melted in our model (compare Figures 1 and 2). This indicates that the GIS in the model of Van Breedam et al. (2020) is closer to instability for pre-industrial climate than in our model.

Using a uniform emission rate during a fixed time interval of 100 years is certainly not representative of the more elongated real anthropogenic CO<sub>2</sub> emissions. However, it allows for a straightforward comparison between different cumulative emission scenarios. Whereas the first several centuries of temperature anomaly and of mass loss of the GIS will be affected by the specific shape of the emission pulse, on a Kyr timescale, mass loss of the GIS is mainly controlled by the cumulative CO<sub>2</sub> emission (e.g., Charbit et al., 2008). In Figure 4, we compare the constant emission rate throughout 100 years as used in our study with a potentially more realistic bell-shaped emission rate. As expected, after approximately 1 Kyr, the effect of the specific emission shape on the volume of the GIS is negligible.

One downside of our approach, in which we employ a fully coupled ESM to model the future evolution of the GIS on multi-millennial timescales, is the computational effort required, therefore necessitating a relatively coarse resolution of 16 km for the ice sheet model. While the resolution is a crucial factor for mass loss of the GIS on centennial timescales, it becomes less important on timescales beyond the millennium (Aschwanden et al., 2019), which is the focus of our study. Finally, we note that we assume an equilibrium pre-industrial GIS, even though Yang et al. (2022) have argued that the past climate could cause a disequilibrium, which may influence future mass loss of the GIS.

## 5. Conclusions

We studied connections between equilibrium states and mass loss of the GIS as a result of anthropogenic CO<sub>2</sub> emissions. We conclude:

- Four equilibrium states of the GIS exist within a global temperature anomaly range between 0 and 2 K relative to pre-industrial. Bifurcation points are found between temperature anomalies of 0.6 and 0.9 K and between 1.6 and 2.0 K.



- System states in the vicinity of the equilibrium ice volumes corresponding to the temperature anomalies right before bifurcation show an increased mass loss rate and an increased sensitivity of mass loss to differences in cumulative CO<sub>2</sub> emission.
- For cumulative emissions larger than 1,000 GtC, the committed sea level from the GIS is 1.8 m. For cumulative emissions larger than 2,500 GtC, almost the complete GIS will be melted in the long term.

### Appendix A: Present-Day Model Performance

An important constraint of the model is its ability to produce a reasonable SMB at present. To this aim we performed a transient historical CLIMBER-X simulation from 1850 to 2015 with prescribed present-day GIS

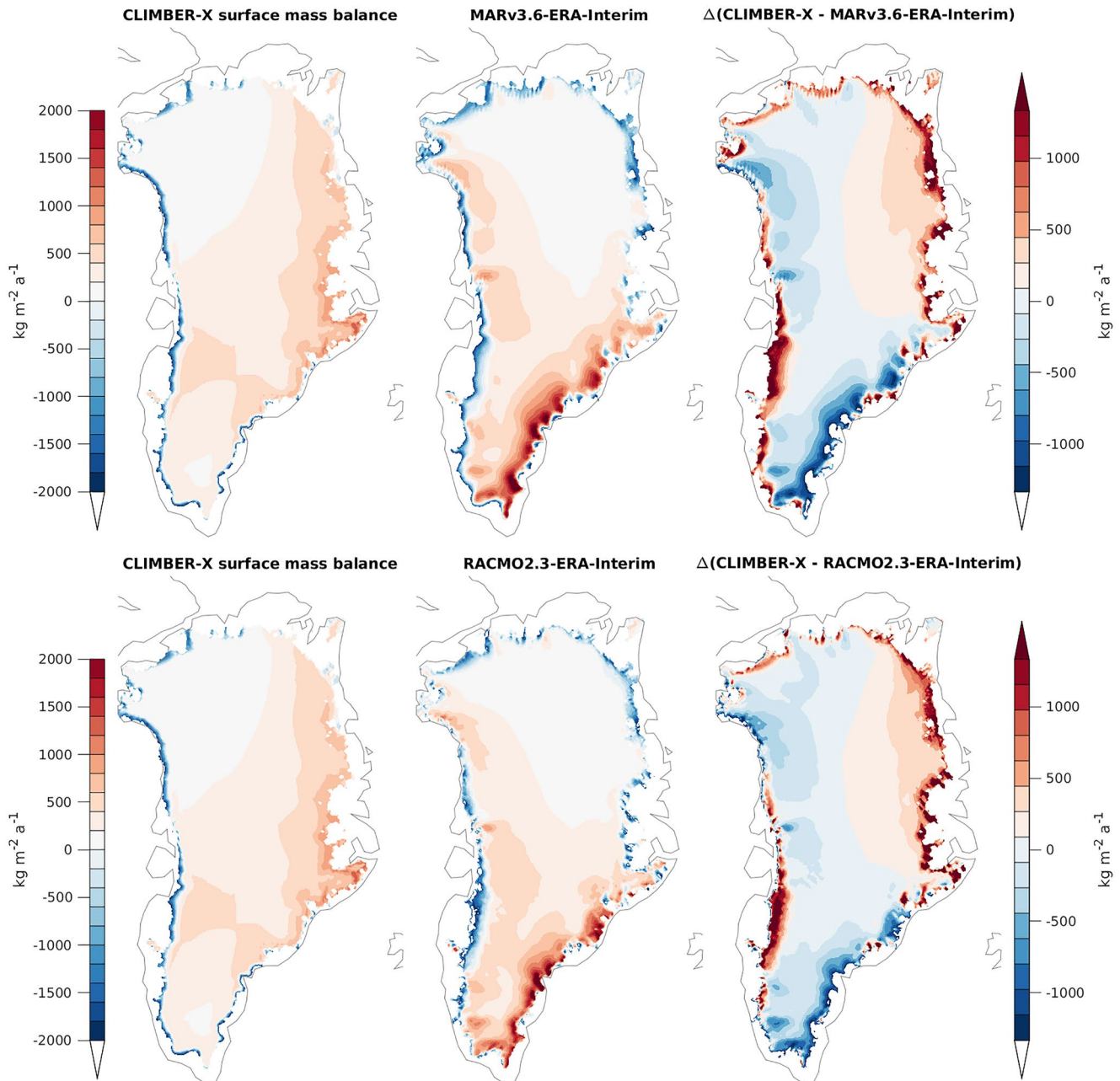


**Figure A1.** Present-day (1981–2010) surface mass balance from a historical CLIMBER-X simulation with prescribed present-day Greenland Ice Sheet (left panels) in comparison to Modèle Atmosphérique Régional (top) and Regional Atmospheric Climate Model (bottom).



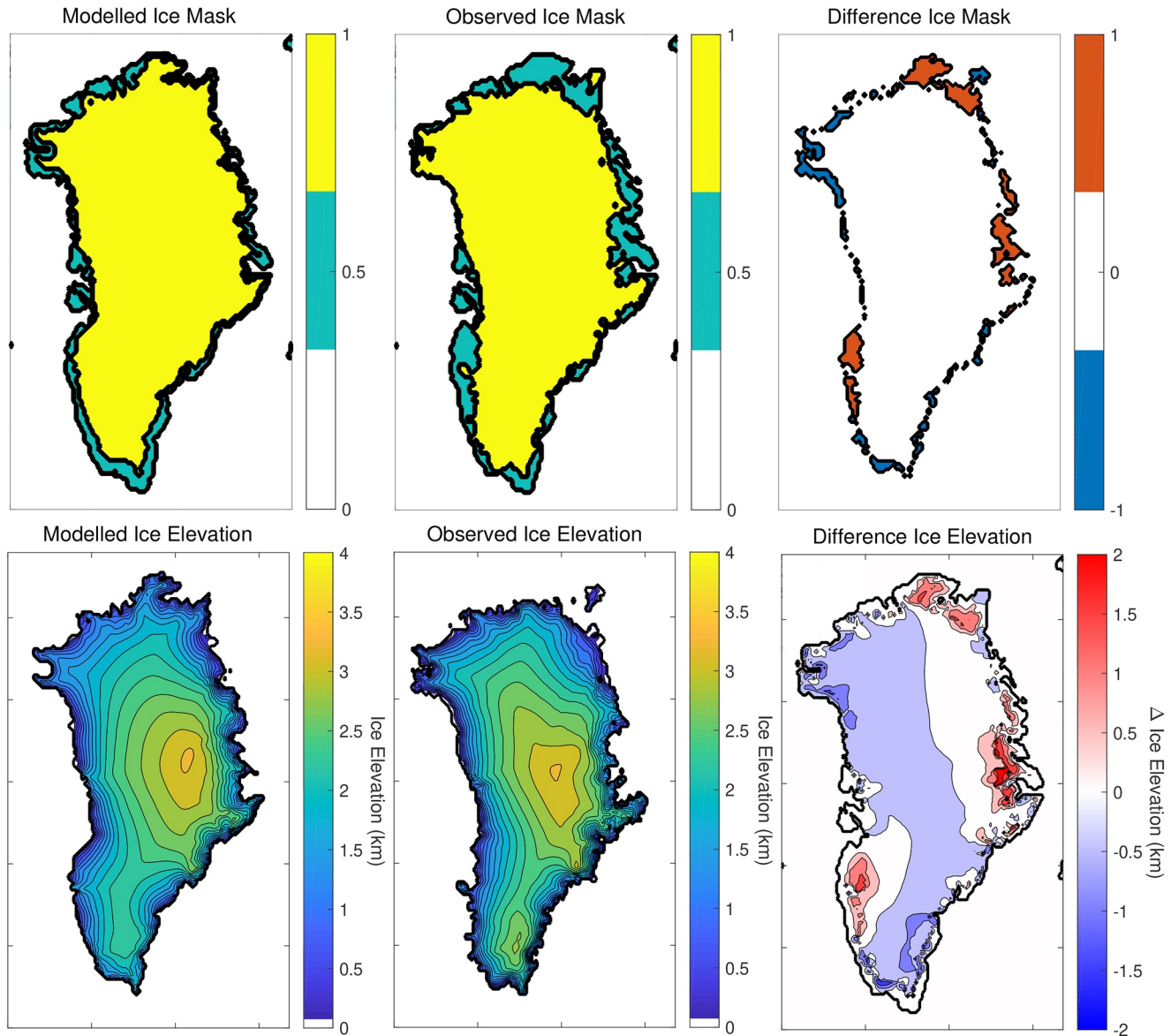


**Figure A2.** Ice mask and elevation comparing the pre-industrial equilibrium Greenland Ice Sheet (GIS) configuration in CLIMBER-X, which is the initial state used in our transient simulations (left) with the observed present-day GIS (Schaffer et al., 2016) (center); differences between model and observations are shown in the right panel (modeled minus observed). In the ice mask plots (top-left and top-center), the value 0 (white) refers to ocean, 0.5 (green) to ice-free land, and 1 (yellow) to ice.

from observations. We then compare the average SMB over the time period 1981–2010 with results from the RCM *Modèle Atmosphérique Régional* (MAR) (Fettweis et al., 2017) and *Regional Atmospheric Climate Model* (RACMO) (Noël et al., 2019) (Figure A1). We find that the margins at the north and west of the GIS have a SMB of  $\approx -500 \text{ kg m}^{-2} \text{ yr}^{-1}$  in all models, while the inner part ranges from zero in the north to slightly positive values in the south. A difference can be identified at the east coast: at the south-east margin, the slightly negative values produced by CLIMBER-X are contrary to the positive values indicated by MAR and RACMO. On the remainder of the east coast, slightly positive values produced by CLIMBER-X are contrary to the slightly negative values produced by MAR and RACMO. The SMB integrated over the ice sheet and averaged over time (1981–2012) produced by CLIMBER-X ( $362 \text{ Gt yr}^{-1}$ ) resembles the values produced by MAR ( $372 \text{ Gt yr}^{-1}$ ) and RACMO ( $357 \text{ Gt yr}^{-1}$ ) (Fettweis et al., 2020) well.

The SMB biases are largely reflected in the shape and elevation of the GIS in pre-industrial equilibrium CLIMBER-X simulations with interactive ice sheets (Figure A2). While the general shape of the GIS is reasonable, the elevation of our pre-industrial GIS, in particular in the south-east, is lower than that observed at present day.

## Data Availability Statement

Produced data are available in Höning et al. (2022).

## Acknowledgments

We thank Andy Aschwanden and an anonymous reviewer for detailed comments that greatly helped us to improve the clarity of the manuscript. We also thank Christine Kaufhold for proofreading the manuscript. DH is funded by the Tipping Points in the Earth System (TIPES) project supported by the European Union's Horizon 2020 research and innovation programme (Grant 820970). MW and MB are funded by the German climate modeling project PalMod supported by the German Federal Ministry of Education and Research (BMBF) as a Research for Sustainability initiative (FONA) (FKZ: 01LP1920B, 01LP1917D and 01LP1918A).

## References

- Applegate, P. J., Parizek, B. R., Nicholas, R. E., Alley, R. B., & Keller, K. (2015). Increasing temperature forcing reduces the Greenland ice sheet's response time scale. *Climate Dynamics*, 45(7), 2001–2011. <https://doi.org/10.1007/s00382-014-2451-7>
- Armstrong McKay, D. I., Staal, A., Abrams, J. F., Winkelmann, R., Sakschewski, B., Loriani, S., et al. (2022). Exceeding 1.5 C global warming could trigger multiple climate tipping points. *Science*, 377(6611), eabn7950. <https://doi.org/10.1126/science.abn7950>
- Aschwanden, A., Fahnestock, M. A., & Truffer, M. (2016). Complex Greenland outlet glacier flow captured. *Nature Communications*, 7(1), 1–8. <https://doi.org/10.1038/ncomms10524>
- Aschwanden, A., Fahnestock, M. A., Truffer, M., Brinkerhoff, D. J., Hock, R., Khroulev, C., et al. (2019). Contribution of the Greenland ice sheet to sea level over the next millennium. *Science Advances*, 5(6), eaav9396. <https://doi.org/10.1126/sciadv.aav9396>
- Bagge, M., Klemann, V., Steinberger, B., Latinović, M., & Thomas, M. (2021). Glacial-isostatic adjustment models using geodynamically constrained 3D Earth structures. *Geochemistry, Geophysics, Geosystems*, 22(11), e2021GC009853. <https://doi.org/10.1029/2021gc009853>
- Bakker, P., Schmittner, A., Lenaerts, J., Abe-Ouchi, A., Bi, D., van den Broeke, M., et al. (2016). Fate of the Atlantic meridional overturning circulation: Strong decline under continued warming and Greenland melting. *Geophysical Research Letters*, 43(23), 12–252. <https://doi.org/10.1002/2016gl070457>
- Bernales, J., Rogozhina, I., Greve, R., & Thomas, M. (2017). Comparison of hybrid schemes for the combination of shallow approximations in numerical simulations of the Antarctic Ice Sheet. *The Cryosphere*, 11(1), 247–265. <https://doi.org/10.5194/tc-11-247-2017>
- Calov, R., Beyer, S., Greve, R., Beckmann, J., Willeit, M., Kleiner, T., et al. (2018). Simulation of the future sea level contribution of Greenland with a new glacial system model. *The Cryosphere*, 12(10), 3097–3121. <https://doi.org/10.5194/tc-12-3097-2018>
- Calov, R., Ganopolski, A., Claussen, M., Petoukhov, V., & Greve, R. (2005). Transient simulation of the last glacial inception. Part I: Glacial inception as a bifurcation in the climate system. *Climate Dynamics*, 24(6), 545–561. <https://doi.org/10.1007/s00382-005-0007-6>
- Calov, R., Robinson, A., Perrette, M., & Ganopolski, A. (2015). Simulating the Greenland ice sheet under present-day and palaeo constraints including a new discharge parameterization. *The Cryosphere*, 9(1), 179–196. <https://doi.org/10.5194/tc-9-179-2015>
- Charbit, S., Paillard, D., & Ramstein, G. (2008). Amount of CO<sub>2</sub> emissions irreversibly leading to the total melting of Greenland. *Geophysical Research Letters*, 35(12). <https://doi.org/10.1029/2008gl033472>
- Choi, Y., Morlighem, M., Rignot, E., & Wood, M. (2021). Ice dynamics will remain a primary driver of Greenland ice sheet mass loss over the next century. *Communications Earth & Environment*, 2(1), 1–9. <https://doi.org/10.1038/s43247-021-00092-z>
- Cierner, C., Winkelmann, R., Kurths, J., & Boers, N. (2021). Impact of an AMOC weakening on the stability of the southern Amazon rainforest. *The European Physical Journal - Special Topics*, 230(14), 3065–3073. <https://doi.org/10.1140/epjs/s11734-021-00186-x>
- Claussen, M., Mysak, L., Weaver, A., Crucifix, M., Fichefet, T., Loutre, M.-F., et al. (2002). Earth system models of intermediate complexity: Closing the gap in the spectrum of climate system models. *Climate Dynamics*, 18(7), 579–586. <https://doi.org/10.1007/s00382-001-0200-1>
- Fettweis, X., Box, J. E., Agosta, C., Amory, C., Kittel, C., Lang, C., et al. (2017). Reconstructions of the 1900–2015 Greenland ice sheet surface mass balance using the regional climate MAR model. *The Cryosphere*, 11(2), 1015–1033. <https://doi.org/10.5194/tc-11-1015-2017>
- Fettweis, X., Hofer, S., Krebs-Kanzow, U., Amory, C., Aoki, T., Berends, C. J., et al. (2020). Grsbmip: Intercomparison of the modelled 1980–2012 surface mass balance over the Greenland ice sheet. *The Cryosphere*, 14(11), 3935–3958. <https://doi.org/10.5194/tc-14-3935-2020>
- Goelzer, H., Nowicki, S., Payne, A., Larour, E., Seroussi, H., Lipscomb, W. H., et al. (2020). The future sea-level contribution of the Greenland ice sheet: A multi-model ensemble study of ISMIP6. *The Cryosphere*, 14(9), 3071–3096. <https://doi.org/10.5194/tc-14-3071-2020>
- Gregory, J. M., & Huybrechts, P. (2006). Ice-sheet contributions to future sea-level change. *Philosophical Transactions of the Royal Society A: Mathematical, Physical and Engineering Sciences*, 364(1844), 1709–1732. <https://doi.org/10.1098/rsta.2006.1796>
- Gregory, J. M., Huybrechts, P., & Raper, S. C. (2004). Threatened loss of the Greenland ice-sheet. *Nature*, 428(6983), 616. <https://doi.org/10.1038/428616a>
- Greve, R. (1997). Application of a polythermal three-dimensional ice sheet model to the Greenland ice sheet: Response to steady-state and transient climate scenarios. *Journal of Climate*, 10(5), 901–918. [https://doi.org/10.1175/1520-0442\(1997\)010<0901:aoptd>2.0.co;2](https://doi.org/10.1175/1520-0442(1997)010<0901:aoptd>2.0.co;2)
- Greve, R., & Blatter, H. (2016). Comparison of thermodynamics solvers in the polythermal ice sheet model sicopolis. *Polar Science*, 10(1), 11–23. <https://doi.org/10.1016/j.polar.2015.12.004>
- Höning, D., Willeit, M., Calov, R., Klemann, V., Bagge, M., & Ganopolski, A. (2022). Data accompanying the paper “multistability and transient response of the Greenland ice sheet to anthropogenic CO<sub>2</sub> emissions” [Dataset]. Zenodo. <https://doi.org/10.5281/zenodo.7515542>
- Huybrechts, P., Goelzer, H., Janssens, I., Driesschaert, E., Fichefet, T., Goosse, H., & Loutre, M.-F. (2011). Response of the Greenland and Antarctic ice sheets to multi-millennial greenhouse warming in the Earth system model of intermediate complexity LOVECLIM. *Surveys in Geophysics*, 32(4), 397–416. <https://doi.org/10.1007/s10712-011-9131-5>
- Irvali, N., Galaasen, E. V., Ninnemann, U. S., Rosenthal, Y., Born, A., & Kleiven, H. K. F. (2020). A low climate threshold for south Greenland ice sheet demise during the late pleistocene. *Proceedings of the National Academy of Sciences*, 117(1), 190–195. <https://doi.org/10.1073/pnas.1911902116>
- Jackson, L., Kahana, R., Graham, T., Ringer, M., Woollings, T., Mecking, J., & Wood, R. (2015). Global and European climate impacts of a slowdown of the AMOC in a high resolution GCM. *Climate Dynamics*, 45(11), 3299–3316. <https://doi.org/10.1007/s00382-015-2540-2>
- Klemann, V., Martinec, Z., & Ivins, E. R. (2008). Glacial isostasy and plate motion. *Journal of Geodynamics*, 46(3–5), 95–103. <https://doi.org/10.1016/j.jog.2008.04.005>
- Martinec, Z., Klemann, V., van der Wal, W., Riva, R., Spada, G., Sun, Y., et al. (2018). A benchmark study of numerical implementations of the sea level equation in GIA modelling. *Geophysical Journal International*, 215(1), 389–414. <https://doi.org/10.1093/gji/ggy280>
- Mottram, R., Simonsen, S. B., Høyer Svendsen, S., Barletta, V. R., Sandberg Sørensen, L., Nagler, T., et al. (2019). An integrated view of Greenland ice sheet mass changes based on models and satellite observations. *Remote Sensing*, 11(12), 1407. <https://doi.org/10.3390/rs11121407>

- Muntjewerf, L., Petrini, M., Vizcaino, M., Ernani da Silva, C., Sellevold, R., Scherrenberg, M. D., et al. (2020). Greenland ice sheet contribution to 21st century sea level rise as simulated by the coupled CESM2.1-CISM2.1. *Geophysical Research Letters*, *47*(9), e2019GL086836. <https://doi.org/10.1029/2019gl086836>
- Noël, B., van de Berg, W. J., Lhermitte, S., & van den Broeke, M. R. (2019). Rapid ablation zone expansion amplifies north Greenland mass loss. *Science Advances*, *5*(9), eaaw0123. <https://doi.org/10.1126/sciadv.aaw0123>
- Noël, B., van de Berg, W. J., Lhermitte, S., Wouters, B., Machguth, H., Howat, I., et al. (2017). A tipping point in refreezing accelerates mass loss of Greenland's glaciers and ice caps. *Nature Communications*, *8*(1), 1–8. <https://doi.org/10.1038/ncomms14730>
- Pattyn, F., Ritz, C., Hanna, E., Asay-Davis, X., DeConto, R., Durand, G., et al. (2018). The Greenland and Antarctic ice sheets under 1.5 C global warming. *Nature Climate Change*, *8*(12), 1053–1061. <https://doi.org/10.1038/s41558-018-0305-8>
- Ridley, J., Gregory, J. M., Huybrechts, P., & Lowe, J. (2010). Thresholds for irreversible decline of the Greenland ice sheet. *Climate Dynamics*, *35*(6), 1049–1057. <https://doi.org/10.1007/s00382-009-0646-0>
- Ritchie, P. D., Clarke, J. J., Cox, P. M., & Huntingford, C. (2021). Overshooting tipping point thresholds in a changing climate. *Nature*, *592*(7855), 517–523. <https://doi.org/10.1038/s41586-021-03263-2>
- Robinson, A., Calov, R., & Ganopolski, A. (2012). Multistability and critical thresholds of the Greenland ice sheet. *Nature Climate Change*, *2*(6), 429–432. <https://doi.org/10.1038/nclimate1449>
- Schaffer, J., Timmermann, R., Arndt, J. E., Kristensen, S. S., Mayer, C., Morlighem, M., & Steinhage, D. (2016). A global, high-resolution data set of ice sheet topography, cavity geometry, and ocean bathymetry. *Earth System Science Data*, *8*(2), 543–557. <https://doi.org/10.5194/essd-8-543-2016>
- Solgaard, A. M., & Langen, P. L. (2012). Multistability of the Greenland ice sheet and the effects of an adaptive mass balance formulation. *Climate Dynamics*, *39*(7), 1599–1612. <https://doi.org/10.1007/s00382-012-1305-4>
- Van Breedam, J., Goelzer, H., & Huybrechts, P. (2020). Semi-equilibrated global sea-level change projections for the next 10 000 years. *Earth System Dynamics*, *11*(4), 953–976. <https://doi.org/10.5194/esd-11-953-2020>
- Vizcaino, M., Mikolajewicz, U., Gröger, M., Maier-Reimer, E., Schurgers, G., & Winguth, A. M. (2008). Long-term ice sheet–climate interactions under anthropogenic greenhouse forcing simulated with a complex Earth system model. *Climate Dynamics*, *31*(6), 665–690. <https://doi.org/10.1007/s00382-008-0369-7>
- Willeit, M., Ganopolski, A., Robinson, A., & Edwards, N. R. (2022). The Earth system model CLIMBER-X v1. 0. Part 1: Climate model description and validation. *Geoscientific Model Development Discussions*, *15*(14), 1–69. <https://doi.org/10.5194/gmd-15-5905-2022>
- Willeit, M., Ilyina, T., Liu, B., Heinze, C., Perrette, M., Heinemann, M., et al. (2023). The Earth system model CLIMBER-X v1. 0—Part 2: The global carbon cycle. *Geoscientific Model Development Discussions*, 1–47.
- Yang, H., Krebs-Kanzow, U., Kleiner, T., Sidorenko, D., Rodehacke, C. B., Shi, X., et al. (2022). Impact of paleoclimate on present and future evolution of the Greenland ice sheet. *PLoS One*, *17*(1), e0259816. <https://doi.org/10.1371/journal.pone.0259816>
- Yu, L., Gao, Y., & Otterå, O. H. (2016). The sensitivity of the Atlantic meridional overturning circulation to enhanced freshwater discharge along the entire, eastern and Western coast of Greenland. *Climate Dynamics*, *46*(5), 1351–1369. <https://doi.org/10.1007/s00382-015-2651-9>